International Journal of Electrical Engineering & Emerging Technology, Vol. 07, No. 01, JUN 2024, pp 08-16

# A Comparison between Normal Quadcopter Configuration & Coaxial Tilt Rotor Tricopter for Visual Inspection Tasks

Muhammad Zulkifal[a,*], Vytautas Bučinskas[b], Vygantas Ušinskis[c], Naimatullah Bhand[d]

[a] *Dipartimento di Ingegneria Meccanica e Aerospaziale, Sapienza Università di Roma - Piazzale Aldo Moro 5, 00185 Roma,Italy*

[b,c] *Department of Mechatronics, Robotics and Digital Manufacturing, Vilnius Gediminas Technical University Lithuania*

[c] *Department of Mechanical Engineering, KU Leuven, Celestijnenlaan 300,B-3001 Heverlee (Leuven)Belgium.*

[*] Corresponding author: Muhammad Zulkifal Email: zulkifal.1995550@studenti.uniroma1.

[**Received on:** 16-04-2024 **Accepted on**: 09-05-2024 **Published on:** 24-06-2024]

***Abstract*** **This paper proposed the comparison between the normal quadcopter configuration with single 4 propellers and Coaxial Tilt Rotor Tricopter for Visual Inspection Tasks, mainly visual inspection of farms for health monitoring.**

**The Design of both configurations is verified and is implemented using the Creo 3d cad software and is simulated in MATLAB/Simulink environment for validation. The hardware is prototyped with the proper choice of Sensors and Actuators like Gyroscope and Accelerometer. The Comparison Analysis also involves Linearization with Estimation algorithm Unscented Kalman Filter(UKF) and Extended Kalman Filter(EKF). Finally, Stability of both configurations are tested with different Robust control Techniques i.e Backstepping.**

***Index Terms*— EKF,UAVs,Tricopter,Kalman filter**

## I. INTRODUCTION

nmanned Aerial Vehicles (UAVs), particularly quadcopters, Uhave revolutionized various industries, notably in performing visual inspection tasks. Their agility and ability to access hard-to-reach areas make them invaluable in applications such as agricultural health monitoring, infrastructure inspection, and surveillance. However, the conventional quadcopter design, while popular, may not always be the most efficient for specific tasks like farm health monitoring. This raises the question of whether alternative UAV configurations could offer superior performance in such applications.

In this context, the Coaxial Tilt Rotor Tricopter (CTRT) emerges as a promising alternative. This research paper presents a comprehensive comparison between the traditional quadcopter configuration and the innovative CTRT, specifically focusing on their effectiveness in visual inspection tasks, with a primary application in farm health monitoring.

To achieve a thorough comparison, both configurations have been meticulously designed using Creo 3D CAD software. This step ensures that each model is optimized for its intended function while adhering to realistic constraints and capabilities. Following the design phase, MATLAB/Simulink simulations provide a robust environment for validating the performance and behavior of these UAVs under various operational conditions. Such simulations are crucial in predicting real-world performance without the risks and costs associated with physical prototyping.

Furthermore, this study goes beyond mere design and simulation. A physical prototype of each configuration has been developed, incorporating essential sensors and actuators like gyroscopes and accelerometers. These components are critical for the UAV's navigation and stability, and their selection and integration are key factors in the overall performance of the UAVs.

The analytical aspect of this research involves a detailed comparison using linearization with advanced estimation algorithms: the Unscented Kalman Filter (UKF) and the Extended Kalman Filter (EKF). These sophisticated algorithms are instrumental in enhancing the UAVs' navigation accuracy and stability, providing a deeper understanding of each configuration's performance.

Lastly, the stability of both configurations under different conditions is rigorously tested using various robust control techniques, with a special emphasis on backstepping. This approach ensures that the UAVs can maintain stable flight and accurate navigation even in challenging conditions, which is paramount for tasks like agricultural health monitoring.

## II. PRELIMINARY DESIGN & ANALYSIS

This flowchart provides a simplified overview of the initial stages of designing a UAV, focusing on the selection and analysis of its structural and power components to ensure it meets performance criteria. Such a process is crucial in designing UAVs that are both efficient and capable of performing their intended tasks effectively.

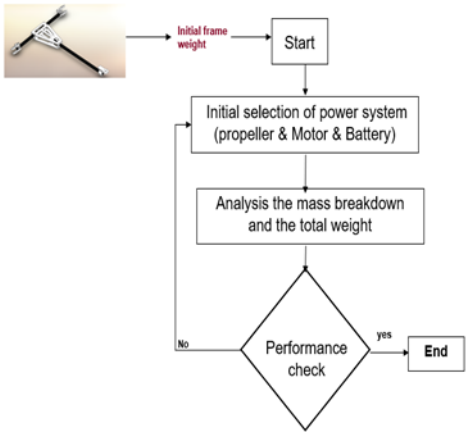


Fig. 1. Flow chart representation of Preliminary Design

Propulsion

A propeller generates thrust from the supplied power, but the magnitude of this force varies. It depends not only on the propeller's rotational speed but also on the velocity of the incoming air. Consequently, propeller tests typically encompass a broad range of operating conditions. This is especially true for APC propellers.below in Fig.2 and Fig.3 illustrates modeling in MATLAB.

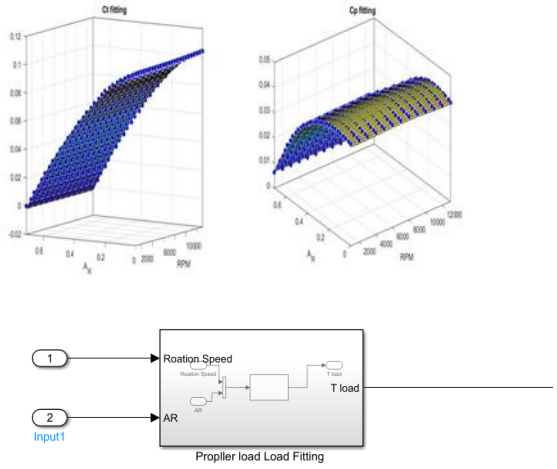


Fig. 2. Modeling in MATLAB

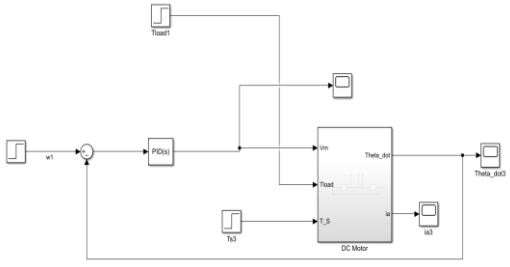


Fig.3. Motor Low level Controller

## III. FINAL SELECTED POWER SYSTEM FOR THE QUADCOPTER

### *A. FOR THE QUADCOPTER*

1- Frame : Hobbypower S500 Quadcopter Fuselage Frame kit PCB version with carbon Fiber landing Gear, 28.7 x 18.29 x 5.33 cm; 530 grams

2- Propeller :1045 10"*4.5" Blade Propeller CW CCW 10inch FPV Probs

3- Brushless Motor : Readytosky 2212 920KV Brushless Motors with 3.5mm bullet connectors, 920rpm/v, DC 7-12V, 4.61 x 4.09 x 1.42 inches, 0.42 Pounds

4- Electronic speed controller: Readytosky 30A ESC 2-60S OPTO Brushless Electronic speed Controller, 30-40A, 28.5g

5- Battery : OVONIC 4s Lipo Battery 5000mAh 50C 14.8V Lipo Battery Hard

Fig.4. Power System for the Quadcopter

We can also Scan market options and the performance Specification of Quadcopter related to market option is shown below in Fig.5.Also Motor specification desired for Quadcopter Applications.

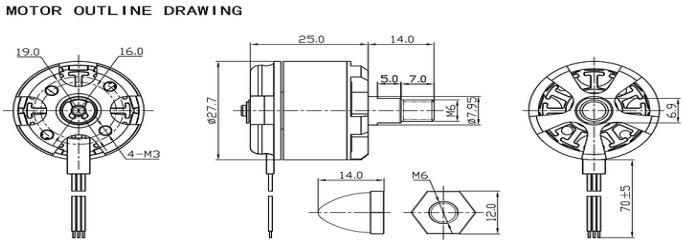


MOTOR PERFORMANCE DATA

| MODEL | KV (rpm/V) | Voltage (V) | Prop | Load Current (A) | Pull (g) | Power (W) | Efficiency (g/W) | Lipo Cell | Weight (g) Approx |
|---|---|---|---|---|---|---|---|---|---|
| B2212 | 920 | 11.1 | 8045 | 7.3 | 465 | 81 | 5.7 | 2-4S | 50 |
| | | | 1045 | 9.5 | 642 | 105 | 6.1 | | |
| | 980 | 11.1 | 8045 | 8.1 | 535 | 90 | 5.9 | | |
| | | | 1045 | 10.6 | 710 | 118 | 6.0 | | |

Fig.5.Motor Performance Data

Total Weight = 1.451 Kg

-Maximum pitch /roll angle by 45 Degree

- Needed Thrust (kg) = $\frac{1.451}{0.707} = 2\ kg$

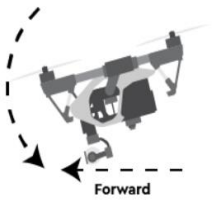


Fig.6. Degree of Freedom Quadcopter

Max Pitch angle =45 Degree

Factor of safety = $\frac{4\times0.642}{2} = 1.28$

*B. FOR THE TRICOPTER*

1- Frame : Designed in soldiworks with a total mass of 310 grams
2- Propeller : Gemfan 5040 for the front propellers . Gemfan 6045 for the tail propellers
3- Brushless Motor : Gemfan M2306L 2200kv Brushless for the Tail propeller ,, Multistar Elite 2306-2150KV Brushless for the front propeller
4- Electronic speed controller: F35A 5S
5- Battery : ZOP Power 14.8V 7500mah 35C 4S Lipo Battery
6- Servo Motor : SUNFOUNDER Servo Motor High Torque Servo, TD8120MG Metal Gear Digital Servo

Fig.7. Power System for the Tricopter

-Total Weight = 1.326 Kg
Factor of safety for producing total thrust for hovering = $\frac{4\times0.33+0.44}{1.326} = 1.328$
estimated flight time while hovering @20.16 A total consumption of five motors = $\frac{7.5}{20.16}\times 60 = 22.32$ min
efficiency drop due to coxail propeller by 20% calculated by this reference [Performance of Coaxial Propulsion in Design of Multi-rotor UAVs
By taking the moment around the CG
Thrust at 10,165 rpm= 0.34
Thrust at 11,755rpm= 0. 162

$$4 \times \text{Thrust}_{\text{front}} \times 0.1 = \text{Thrust}_{\text{tail}} \times 0.2$$
$$4 \times 0.\ 162 \times 0.1 = 0.34\ \times 0.2$$

| Number | Compenent | Mass (kg) | | Percenateg | |
|---|---|---|---|---|---|
| | | Quadcopter | Tricopter | Quadcopter | Tricopter |
| 1 | Frame | 0.53 | 0.38 | 36.96% | 28.66% |
| 2 | Motors | 0.128 | 0.13 | 8.93% | 9.80% |
| 3 | batteries | 0.508 | 0.571 | 35.43% | 43.06% |
| 4 | ECS | 0.153 | 0.05 | 10.67% | 3.77% |
| 5 | Autopolit | 0.015 | 0.015 | 1.05% | 1.13% |
| 6 | camera | 0.1 | 0.1 | 6.97% | 7.54% |
| 7 | Servo actuation | 0 | 0.08 | 0.00% | 6.03% |
| 8 | Total Weigth | 1.434 | 1.326 | | |

Fig.8. Performance Specification for Tricopter

## IV. MASS BREAK DOWN

In both tricopters and quadcopters, key components include the lightweight frame, motors, propellers, electronic speed controllers (ESCs), flight controller, and battery. Electronic components such as gyroscopes, accelerometers, and GPS modules aid in stabilization and navigation. Payload, like cameras or sensors, may also be added. Optimization of these components ensures efficient flight performance and maneuverability while carrying out specific tasks such as aerial photography or surveillance.

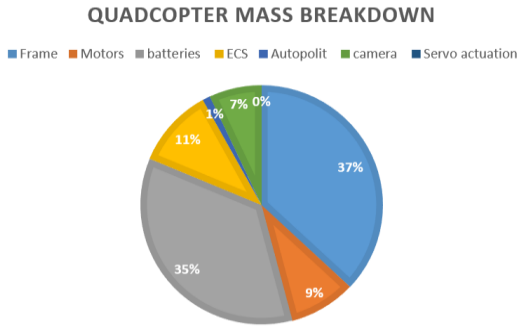


Fig.9.Quadcopter mass Breakdown

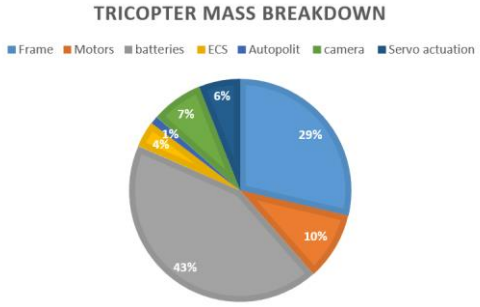


Fig.10. Tricopter mass Breakdown

## V. CAD DESIGN

Below represent the CAD model calculations for Quadcopter and Tricopter

Total dimensions :length= 40 cm

Width=53 cm Height= 22 cm

Moment of inertia = $I_{xx} = 1.2 \times 10^{-2} = I_{yy} = 1.03 \times 10^{-2} = I_{zz} = 2.11 \times 10^{-2}$

CG location to the tail = 20 cm

Total Mass= 1.215 kg

Aerodynamic Forces

Total dimensions :length= 50 cm Width= 50 cm Height = 22 cm

Moment of inertia = $I_{xx} = 2.13 \times 10^{-2} = I_{yy} = 2.217 \times 10^{-2} = I_{zz} = 2.82\ \times 10^{-2}\ in\ kg.m^2$

CG location = exactly in the middle

Total Mass= 1.456 kg

Fig.11.Final CAD Model left Tricopter and right Quadcopter

### A. *Aerodynamic Forces*

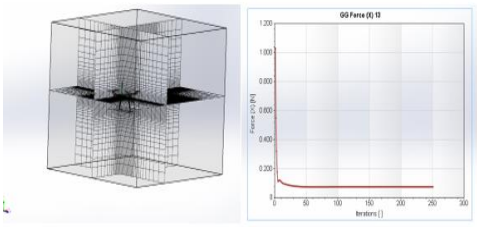

Fig.12.Aerodynamics forces

With the geometry, to obtain realistic aerodynamic coefficients such as drag and lift coefficient.

we study our model with CFD simulations, with propellers kept fixed for the sake of simplicity. We decided to perform drag coefficients for the 3 body axis directions, and so with fluid coming from X, then Y and Z, for different kind of velocities: for this kind of geometry, lift coefficient are negligible w.r.t drag. Moreover, the coefficients were more or less constant w.r.t velocity.Fig.13 and Fig.14 shows Comparison between the aerodynamics coefficients

Fig.13.Tricopter Aerodynamics Forces

The coefficient of drag in X direction = 0.0736

The coefficient of drag in Y direction = 0.04929

The coefficient of drag in Z direction = 0.0342

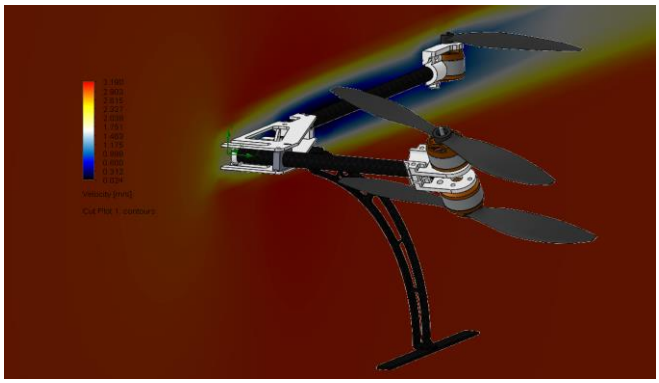

Fig.14.Quadcopter Aerodynamics Forces.

The coefficient of drag in X direction = 0.06277

The coefficient of drag in Y direction = 0.03221

The coefficient of drag in Z direction = 0.04952

The Lift coefficient is negligible in both cases

## VI. DYNAMIC MODELING

### A. *QUADCOPTER*

*Variables descriptions:*

$w_i (i = 1 \dots 4)$ are rotational speed of 4 rotors
F is the net force acting on quadcopter
$1_3$ is the identity matrix
a is the linear acceleration
$I_3$ is the moment of inertia
$v$ is the linear velocity
$\tau$ is the net torque
$\alpha$ is angular acceleration

$$\begin{bmatrix} F \\ \tau \end{bmatrix} = \begin{bmatrix} m1_3 & 0_3 \\ 0_3 & I_3 \end{bmatrix} \begin{bmatrix} a \\ \alpha \end{bmatrix} + \begin{bmatrix} 0 \\ \omega \times I_3 \omega \end{bmatrix}$$

$T = f_1 + f_2 + f_3 + f_4$, $f_i = b w_i^2 \quad i = 1, \dots, 4$ (b is a thrust factor) and $\tau_{R,i} = d w_i^2$ in which d is drag factor

$$\sum F_I = \begin{pmatrix} 0 \\ 0 \\ mg \end{pmatrix} + I_{R_B}(\varphi, \theta, \psi) \begin{pmatrix} 0 \\ 0 \\ -T \end{pmatrix} + F_A + F_D$$

$$\sum F_I = \begin{pmatrix} L_\varphi \\ L_\theta \\ L_\psi \end{pmatrix} + \begin{pmatrix} \tau_\varphi \\ \tau_\theta \\ \tau_\psi \end{pmatrix} + \tau_A + \tau_D$$

In quadcopter we have 4 control inputs which are F in z direction and 3 moment inputs.

$$m\ddot{P} = \begin{bmatrix} 0 \\ 0 \\ mg \end{bmatrix} + R_{gb} \begin{bmatrix} 0 \\ 0 \\ -T \end{bmatrix} + F_A + F_D$$

$$\ddot{x} = -(cos_\psi sin_\theta cos_\phi + sin_\psi sin_\phi) \frac{T}{m}$$

$$\ddot{y} = -(sin_\psi sin_\theta cos_\phi + sin_\psi cos_\phi) \frac{T}{m}$$

$$\ddot{z} = g - cos_\theta cos_\phi \frac{T}{m}$$

$P = [x \ y \ z]^T$ , P denotes the position w.r.t inertia frame
$\phi$, $\theta$ and $\psi$ denote the angle of roll, pitch and yaw w.r.t the inertial frame, respectively.
m is mass and g is gravity
$T = f_1 + f_2 + f_3 + f_4$
Assumptions: there are aerodynamics ($F_A$) and disturbances ($F_D$) $\quad F_A = \frac{1}{2} \rho A v^2$

$\Omega = [p \ \ q \ \ r]^T$ ($p, q$ and $r$ denote the angular velocity of roll, pitch and yaw)

$$\Theta = [\phi \ \ \theta \ \ \psi]^T$$

$$\begin{cases} \dot{\Theta} = T(\Theta)\Omega \\ I\dot{\Omega} = M - \Omega \times (I\Omega) \\ M = G_a + \tau + M_{anti} \end{cases}$$

$$\ddot{\phi} = \frac{1}{I_{xx}} \tau_{bx}$$

$$\ddot{\theta} = \frac{1}{I_{yy}} \tau_{by}$$

$$\ddot{\psi} = \frac{1}{I_{zz}} \tau_{bz}$$

$$I\begin{bmatrix}\dot{p}\\ \dot{q}\\ \dot{r}\end{bmatrix}=\begin{bmatrix}\tau_{bx}\\ \tau_{by}\\ \tau_{bz}\end{bmatrix}-\begin{bmatrix}p\\ q\\ r\end{bmatrix}\times I\begin{bmatrix}p\\ q\\ r\end{bmatrix}$$

Rotors have the same rotation speed and opposite directions so, the gyroscopic moment and reaction torque are counteracted in the hovering case.
We have symmetric shape
$M_{anti}$ is the reaction torque vector and $G_a$ is gyroscopic moment.

### B. TRICOPTER

*Variables descriptions*:
$w_i(i=1\dots5)$ are rotational speed of 5 rotors

$$w_2=w_3,\ w_4=w_5$$

$\alpha_r and\ \alpha_l$ are tilt angles of right and left coaxial rotors
$c_t\ and\ c_m$ are thrust and torque coefficient
$F_{bx}\ and\ F_{bz}$are forces along direction
$x_b\ and\ z_b$, respectively
$\tau_{bx}, \tau_{by}$ and $\tau_{bz}$ are torques generated by imbalance of the thrust w.r.t body frame.
The control allocation is given by:

$$\begin{bmatrix}F_{bx}\\ F_{bz}\\ \tau_{bx}\\ \tau_{by}\\ \tau_{bz}\end{bmatrix}=\begin{bmatrix}0 & 0 & 2c_t & 0 & 2c_t\\ -c_t & -2c_t & 0 & -2c_t & 0\\ 0 & -2c_m l_3 & 0 & 2c_m l_3 & 0\\ -c_m l_1 & 2c_m l_2 & 0 & 2c_m l_3 & 0\\ 0 & 0 & -2c_m l_3 & 0 & 2c_m l_3\end{bmatrix}\begin{bmatrix}w_1^2\\ w_2^2 cos_{\alpha_r}\\ w_2^2 sin_{\alpha_r}\\ w_4^2 cos_{\alpha_l}\\ w_4^2 sin_{\alpha_l}\end{bmatrix}$$

In tricopter we have 5 control inputs which are $F_{bx}\ and\ F_{bz}$ and 3 moment inputs. $F_{bx}$ coming from the tilting of the rotors

$$m\ddot{P}=\begin{bmatrix}0\\ 0\\ mg\end{bmatrix}+R_{gb}\begin{bmatrix}F_{bx}\\ 0\\ F_{bz}\end{bmatrix}+F_A+F_D$$

$$\ddot{x}=\left(cos_\psi sin_\theta cos_\phi+sin_\psi sin_\phi\right)\frac{F_{bz}}{m}+\frac{F_{bx}}{m}cos_\theta cos_\psi$$

$$\ddot{y}=\left(sin_\psi sin_\theta cos_\phi+cos_\psi sin_\phi\right)\frac{F_{bz}}{m}+\frac{F_{bx}}{m}cos_\theta sin_\psi$$

$$\ddot{z}=g+cos_\theta cos_\phi\frac{F_{bz}}{m}-sin_\theta\frac{F_{bx}}{m}$$

$P=[x\ \ y\ \ z]^T$, P denotes the position w.r.t inertia frame
$\Theta=[\phi\ \ \theta\ \ \psi]^T$ where $\phi$, $\theta$ and $\psi$ denote the angle of roll, pitch and yaw w.r.t the inertial frame, respectively.
m is mass and g is gravity
Assumptions: there are aerodynamics ($F_A$) and disturbances ($F_D$)
$F_A=\frac{1}{2}\rho A v^2$
$\Omega=[p\ \ q\ \ r]^T$ ($p, q\ and\ r$ denote the angular velocity of roll, pitch and yaw)

$$\Theta=[\phi\ \ \theta\ \ \psi]^T$$

$M_{anti1}=[0\ \ 0\ \ -c_m {w_1}^2]^T$

$$G_{a1}=J_1[-q\ \ p\ \ 0]^T$$

$$\begin{cases}\dot{\Theta}=T(\Theta)\Omega\\ I\dot{\Omega}=M-\Omega\times(I\Omega)\\ M=G_a+\tau+M_{anti}\end{cases},\ M=[M_{bx}\ \ M_{by}\ \ M_{bz}]$$

(M is the moment)

$$\ddot{\phi}=\frac{1}{I_{xx}}\tau_{bx}+\frac{1}{I_{xx}}(I_{yy}-I_{zz})\dot{\theta}\dot{\psi}$$

$$\ddot{\theta}=\frac{1}{I_{yy}}\tau_{by}+\frac{1}{I_{yy}}(I_{zz}-I_{xx})\dot{\phi}\dot{\psi}$$

$$\ddot{\psi}=\frac{1}{I_{zz}}\tau_{bz}+\frac{1}{I_{zz}}(I_{xx}-I_{yy})\,\dot{\phi}\,\dot{\theta}$$

$$I\begin{bmatrix}\dot{p}\\ \dot{q}\\ \dot{r}\end{bmatrix}=\begin{bmatrix}\tau_{bx}\\ \tau_{by}\\ \tau_{bz}\end{bmatrix}-\begin{bmatrix}p\\ q\\ r\end{bmatrix}\times I\begin{bmatrix}p\\ q\\ r\end{bmatrix}$$

$M_{anti}$ is the reaction moment and $G_a$ is gyroscopic moment.
Coaxial rotors have the same rotation speed and opposite directions so, the gyroscopic moment and reaction torque are counteracted so we only consider rotor 1.
$M_{anti1}$ and $G_{a1}$ are regarded as disturbances here.
$\tau=[\tau_{bx}\ \tau_{by}\ \ \tau_{bz}]^T$ $\tau$ is the torque generated by rotor thrust

## VII. SENSOR SELECTION

To find the position of Tricopter/Quadcopter, the MPU-6050 devices combine a 3-axis gyroscope and a 3-axis accelerometer in a closed architecture chip, together with an onboard Digital Motion Processor™ (DMP™), which can filter the data and process complex calculations quickly.

The data is transferred using an I2C bus to the microcontroller from MPU6050.

One of the disadvantage of gyroscopes is their sensitivity to vibrations. This can be a problem in a tricopter, taking into account the change of one's tilting, can create vibrations in the body of the vehicle. To reduce this noise, the MPU-6050 is mounted between a soft shock absorbing material that protects it from of the vibration.

An important feature of a gyroscope and its selection criterion for the intended application corresponds to how fast the sensor can perceive. The MPU-6050 used in the tricopter has four sensitivity settings that the user can select

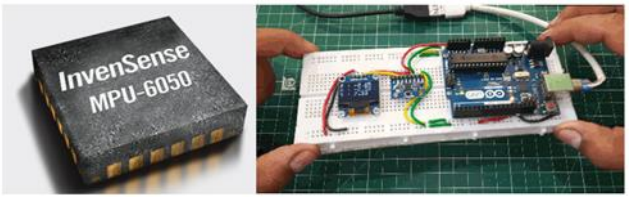

Fig.15.Sensors Modeling

### A. Gyroscope

A gyroscope sensor is an instrument capable of measuring and preserving an object's orientation and angular velocity. The MEMS sensor comprises a mass (divided into four parts: M1, M2, M3, and M4) that is perpetually oscillated to respond to the Coriolis effect. These components move simultaneously inward and outward within the horizontal plane. The sensor operates in three distinct modes, determined by the axis along which angular rotation is applied.


Fig.16.Gyroscope position orientations

### B. *Accelerometer*

The Accelerometer is a sensor that measures acceleration, that is, the change in speed in time.
This structure is suspended by polysilicon springs. It allows the structure to deflect at the time when the acceleration is applied on the particular axis.
Due to deflection the capacitance between fixed plates and plates attached to the suspended structure is changed. This change in capacitance is proportional to the acceleration on that axis.
The sensor processes this change in capacitance and converts it into an analog output voltage.
If Tricopter/Quadcopter lifts up, then the accelerometer reads a positive value. If Tricopter/Quadcopter goes down, then the accelerometer reads a negative value.
Sensor fusion techniques integrate sensory data to produce information with reduced uncertainty and increased accuracy. This integration of sensor outputs is achieved through the implementation of filters such as the Kalman filter or the complementary filter

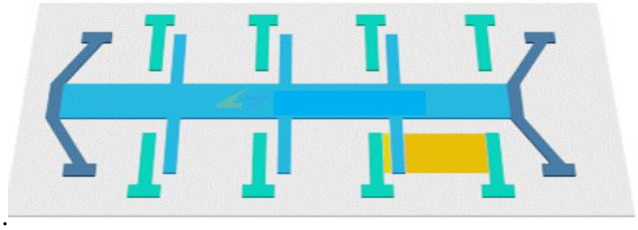

Fig.17.Accelerometer

## VIII. Controllability and Observability

Because of under actuation our system is not fully controllable (we have 5 control while 6 degrees of freedom). Our system is fully observable so we can reconstruct all the states using Kalman filter.

### C. *Unscented Kalman Filter(UKF) and Extended Kalman Filter(EKF)*

*1) Position Discretised Dynamics:*

$$x_1(k+1) = x_1(k) + x_2T_s\,,\ \dot{x}_1 = x_2$$

$$X_2(k+1) = x_2(k) + \left(\frac{1}{m}cos\theta cos\psi\right)u(1) + \frac{1}{m}(sin\theta cos\psi cos\Phi) + (sin\psi sin\phi u(2))T_S$$

$$X_3(k+1) = x_3(k) + x_4T_S$$

$$X_4(k+1) = x_4(k) + \left(\frac{1}{m}cos\theta sin\psi\right)u(1) + \frac{1}{m}(sin\theta sin\psi cos\Phi) - (cos\psi sin\phi u(2))T_S$$

$$X_5(k+1) = x_5(k) + x_6T_S$$

$$X_6(k+1) = x_6(k) + (g - \frac{1}{m}sin\theta u(1)) + \frac{1}{m}cos\theta cos\phi u(2)T_S$$

*2) Rotations Discretised Dynamics:*

$$x_7(k+1) = x_7(k) + x_8T_s\,,\ \dot{x}_7 = x_8$$

$$x_8(k+1) = x_8(k) + (\frac{1}{I_{xx}}(I_{yy} - I_{zz})x(10)x(12) + \frac{1}{I_{xx}}u(3))T_s$$

$$x_9(k+1) = x_9(k) + x_{10}T_s$$

$$x_{10}(k+1) = x_{10}(k) + (\frac{1}{I_{yy}}(I_{zz} - I_{xx})x(8)x(12) + \frac{1}{I_{yy}}u(4))T_s$$

$$x_{11}(k+1) = x_{11}(k) + x_{12}T_s$$

$$x_{12}(k+1) = x_{12}(k) + (\frac{1}{I_{zz}}(I_{xx} - I_{yy})x(8)x(10) + \frac{1}{I_{zz}}u(5))T_s$$

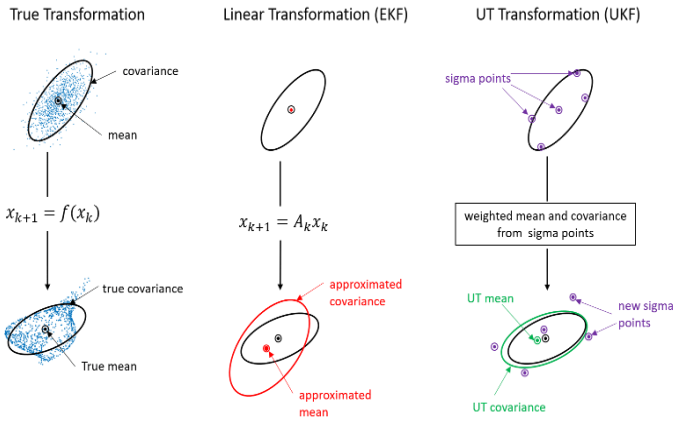


Fig.18.Unscented Kalman Filtering

## IX. Tuning the Parameters

We assume: Q=0.003, R=1e-6 (Q and R correspond to the process and measurement noise covariance matrices).
We consider Zero mean, white Gaussian additive noise for process noise and Zero mean, white Gaussian additive noise for measurement.

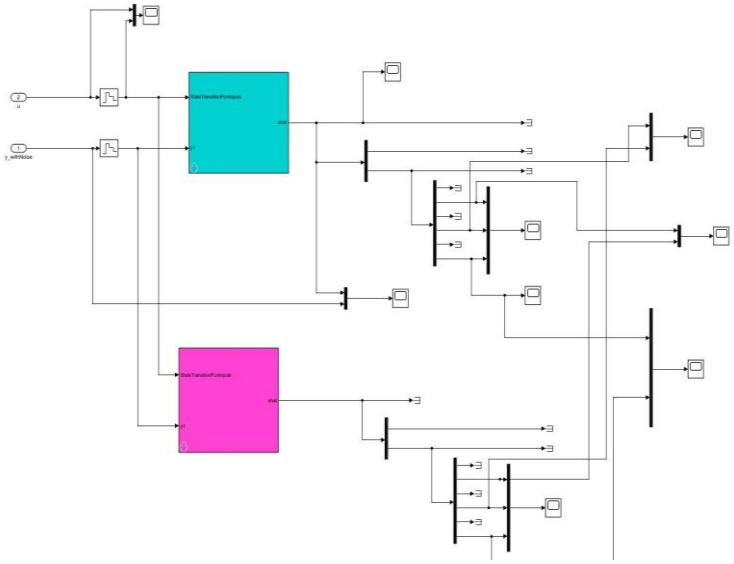

Fig.19.Simulink Modeling

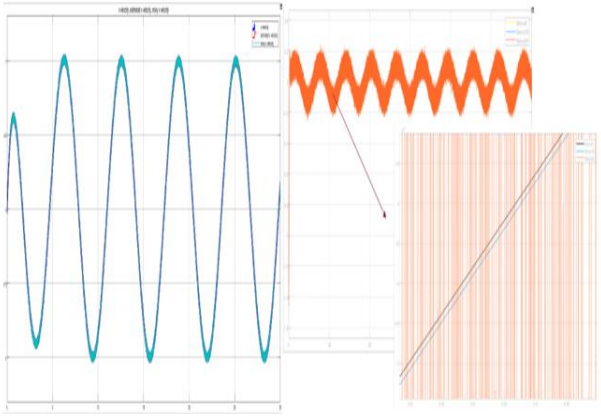

Fig.20.Simulink results

Fig.20.General Overview with Simulink implementaion

## X. THE CONTROL METHODOLOGY

Due to the under actuation that is present in both the quadcopter and the tricopter systems, a hierarchical control architecture has been proposed.
In fact, both the multirotor would like to move and rotate in the 6 DOFs but they have a smaller number of control inputs (4 for the quadrotor and 5 for the tricopter).
This from a control perspective will imply that we can track only 4 and 5 references respectively, unless we use more complex control architectures, like a hierarchical one.
Moreover, due to the tilting rotors, the tricopter can perform a direct translation along the x-axis, that is not possible for the quadcopter due to harder under actuation.

In this paper I will mainly address the control strategy proposed for the tricopter. We have implemented a hierarchical backstepping sliding mode controller for the nonlinear system without linearization around operating conditions (trimming).

The control scheme is like the classical quadrotor's one, but thanks to the extra control input due to the tilting of the rotors, the position controller compute only the desired roll angle $\varphi_d$ and the corresponding the angular speed. This will allow us to specify two angular references instead of one: one for the yaw $\psi_d$, and the other for the pitch $\theta_d$.

The P.C. compute also the forces in the body frame along x and z axis, while the inner and faster A.C. generate the control torques.

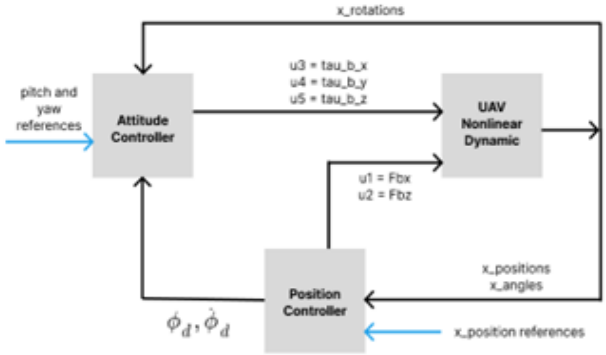


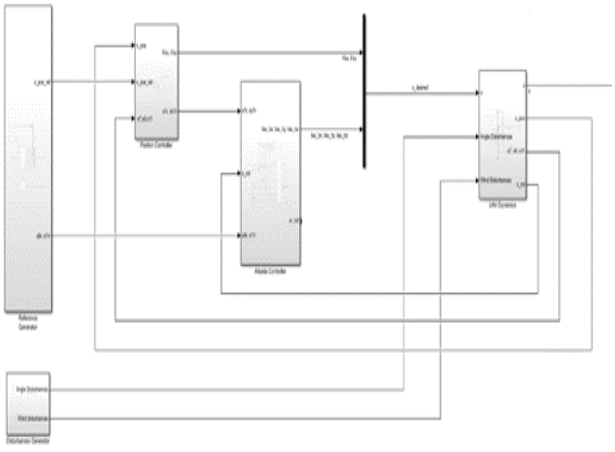

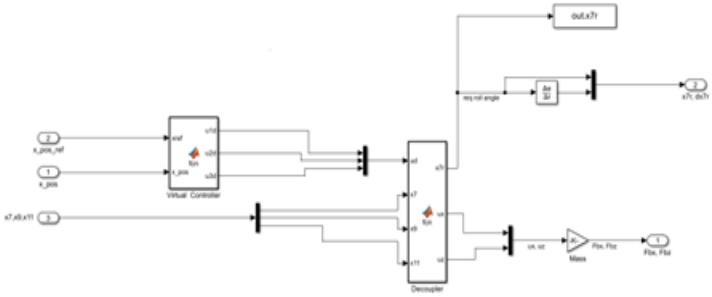

Fig.21.Position Controller

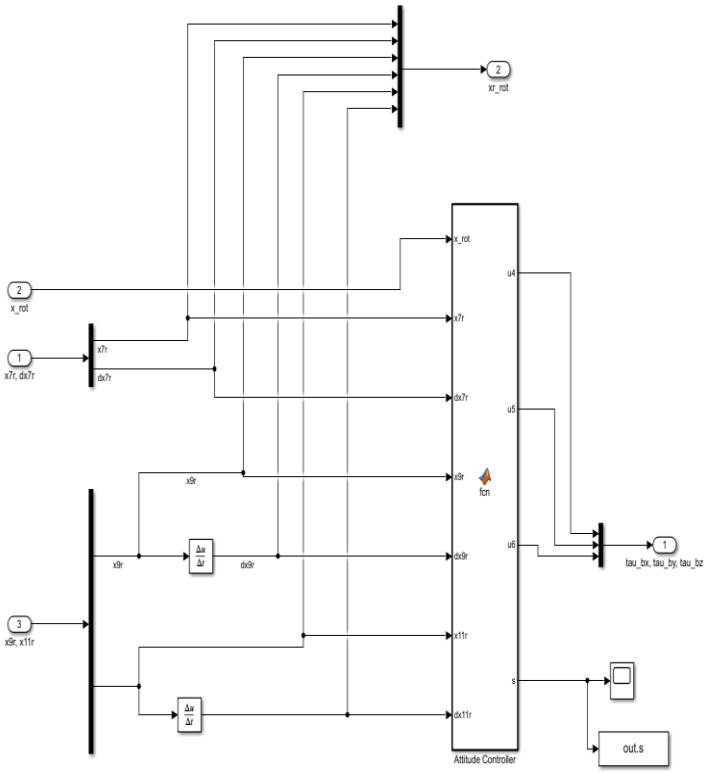


Fig.22.Attitude Controller

## XI. SIMULATION AND RESULTS

The reference trajectories I tested the model along 3 different trajectories:
1. Hovering
2. Constant altitude tracking + ramp position reference along x-axis
3. Helix

I also specified a fixed reference for the yaw equal to zero, and the same for the pitch.
A constant wind disturbance is always applied.
In order to isolate the effects of the disturbances on the reference tracking, we applied the roll, pitch and yaw disturbances respectively at 10, 20 and 30 seconds from the beginning of the simulations.

*I. Trajectory 1: Hovering*

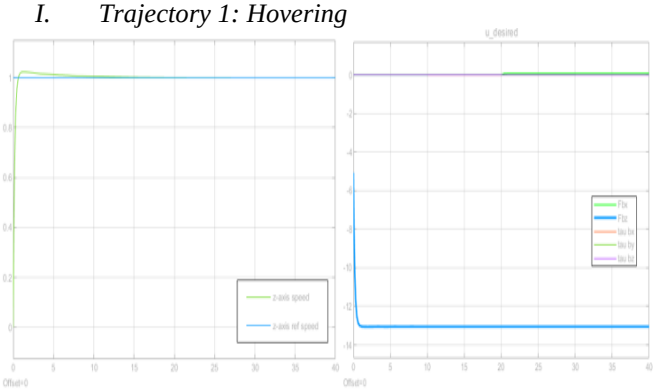

Fig,23. a)Robot's velocity along z-axis b)Control inputs

*II. Trajectory 2: Constant altitude + ramp position reference along x-axis*

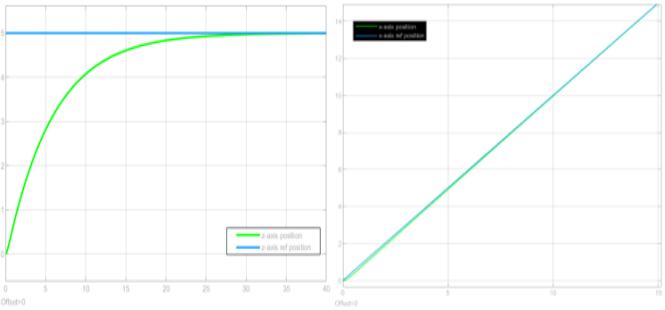

Fig.24.a) Robot's position along z-axis b) Robot's position along x-axis

*III. Trajectory 2: Constant altitude + ramp position reference along x-axis*

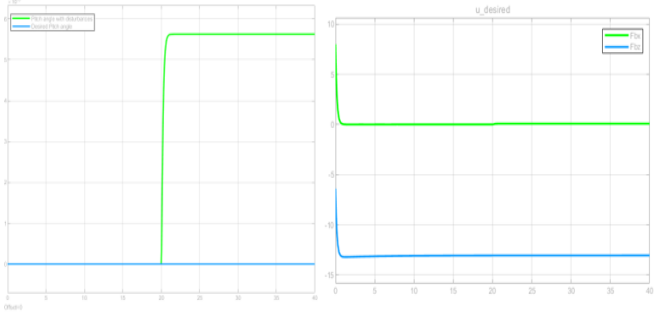

Fig.25.Pitch angle (with disturbances b) Control inputs

*IV. Trajectory 3: Helix*

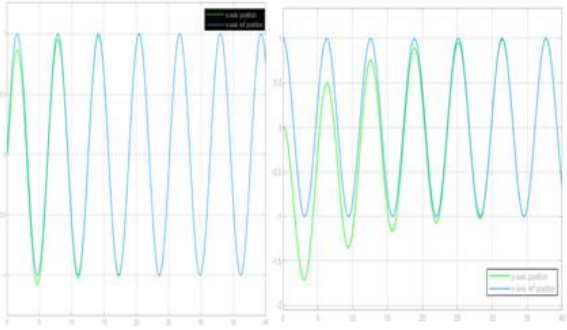

Fig.26.a) Robot's position along x-axis b) Robot's position along y-axis

*V. Trajectory 3: Helix*

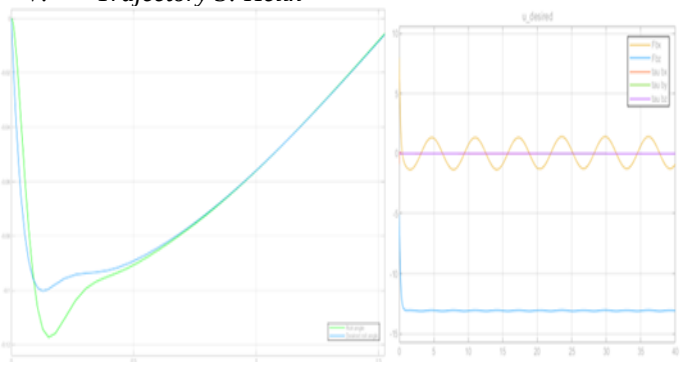

Fig.27.a)Desired roll angle tracking b)Control effort

*VI. Trajectory 3: Helix*

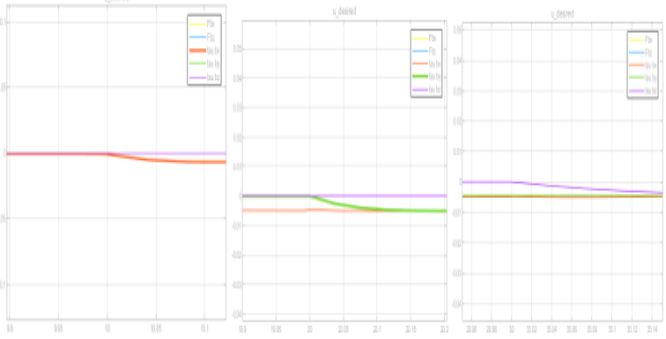

**a)** Roll disturbance (10 s) Torque control input around x-axis start counteracting
**b)** Pitch disturbance (20 s) Torque control input around y-axis start counteracting
**c)** Yaw disturbance (30 s) Torque control input around z-axis start counteracting

## XII. CONCLUSION

The meticulously selected components outlined for the quadcopter, from the SolidWorks-designed frame to the Gemfan propellers, and the carefully chosen brushless motors, electronic speed controller, battery, and servo motor, represent a finely tuned system engineered for optimal performance. Each component contributes to the quadcopter's stability, agility, and efficiency, ensuring it is well-equipped to excel in a variety of aerial applications. This comprehensive approach to component selection and integration underscores the quadcopter's versatility and reliability, making it a valuable asset for tasks ranging from aerial photography to surveillance.

## XIII. REFERENCES

[1] Robust backstepping sliding mode control for coaxial tilt-rotor UAV
(2022 5th International Symposium on Autonomous Systems (ISAS))
[2] He, Guang & Yu, Li & Huang, Huaping & Wang, Xiangke. (2020). A Nonlinear Robust Sliding Mode Controller with Auxiliary Dynamic System for the Hovering Flight of a Tilt Tri-

Rotor UAV. Applied Sciences. 10. 6551. 10.3390/app10186551.
[3] Alexis,K.;Nikolakopoulos,G.;Tzes,A.Model predictive control scheme for the autonomous flight of an unmanned quadrotor.In Proceedings of the 2011 IEEE International Symposium on Industrial Electronics,Gdansk,Poland,27–30June2011;pp.2243–2248

[4] Rendón, M.A.; Martins, F.F. Unmanned quadrotor path following nonlinear control tuning using particle swarm optimization. In Proceedings of the 2018 Latin American Robotic Symposium, 2018 Brazilian Symposium on Robotics (SBR) and 2018 Workshop on Robotics in Education (WRE), Joao Pessoa, Brazil, 6–10 November 2018; pp. 509–514.

[5] Bianchi, D.; Di Gennaro, S.; Di Ferdinando, M.; Acosta Lùa, C. Robust Control of UAV with Disturbances and Uncertainty Estimation. Machines 2023, 11, 352.

[6] Altan, A.; Aslan, Ö.; Hacıoˇ glu, R. Model reference adaptive control of load transporting system on unmanned aerial vehicle. In Proceedings of the 2018 6th International Conference on Control Engineering & Information Technology (CEIT), Istanbul, Turkey, 25–27 October 2018; pp. 1–5.
[7] Eltayeb, A.; Rahmat, M.F.; Basri, M.A.M.; Eltoum, M.M.; El-Ferik, S. An improved design of an adaptive sliding mode controller for chattering attenuation and trajectory tracking of the quadcopter UAV. IEEE Access 2020, 8, 205968–205979.
[8] Mofid,O.; Mobayen, S. Adaptive sliding mode control for finite-time stability of quad-rotor UAVs with parametric uncertainties. ISA Trans. 2018, 72, 1–14.
[9] Zhen, Z.; Tao, G.; Xu, Y.; Song, G. Multivariable adaptive control based consensus flight control system for UAVs formation. Aerosp. Sci. Technol. 2019, 93, 105336.
[10] Kennedy, J.; Eberhart, R. Particle swarm optimization. In Proceedings of the ICNN'95-International Conference on Neural Networks, Perth, WA, Australia, 27 November–1 December 1995; Volume 4, pp. 1942–1948
.[11]Moon,J.S.;Kim,C.;Youm,Y.;Bae,J.UNI-Copter:Aportablesingle-rotor powered spherical unmanned aeria lvehicle(UAV) with an easy-to-assemble and flexible structure. J.Mech.Sci.Technol.2018,32,2289–2298.